K. Ganesh Kumar, G.K. Ramesh*, B.J. Gireesha, and A.M. Rashad

On stretched magnetic flow of Carreau nanofluid with slip effects and nonlinear thermal radiation

https://doi.org/10.1515/nleng-2017-0120
Received August 13, 2017; revised January 28, 2018; accepted April 7, 2018.

Abstract: Present article reports the magnetohydrodynamic flow of Carreau nanofluid in the presence of nonlinear thermal radiation. In this model we incorporated slip condition on heat and mass boundary conditions. Similarity transformations are applied to convert the governing dimensional expressions into non-dimensional forms. Runge-Kutta-Fehlberg method of fourth–fifth order using shooting technique utilized to elaborate the numerical solutions of physical phenomenon.A comparative analysis is presented with the previous published data in special case for the justification of present results. The role of physical constraints on liquid velocity, temperature and concentration are discussed through numerical data and plots.

Keywords: Carreau nanofluid, thermal and solutal slip, nonlinear radiation, magnetic field

1 Introduction

Convective heat transport is a fundamental aspect of various industrial operations. The efficiencies of thermal devices and systems are related to heat transfer rates which in turn depend on the thermal conductivity of the working fluids. With increasingly more sophisticated improvements in nanotechnology and optimization, the request is increasing for more effective and durable heat transfer fluids with significantly greater thermal conductivities than traditional ones. Traditional heat transfer fluids (water, oils and ethylene glycol) applied in the currently thermal systems have relatively low thermal conductivities compared to solids. Nanofluids, an enterprising and clearly more efficient kind of working fluid, are gained by dissolving nanometer-sized particles/fibers between 1 and 100 nm in traditional heat transfer fluids. An excellent literature review on nanofluids transport phenomena and their different applications is reported in Das et al. [1] and Choi [2]. Nield and Kuznetsov [3] used the mathematical nanofluid model suggested by Buongiorno [4] to examine the influence of Brownian motion and thermophoresis on nanofluid natural convection flow over a vertical plate under the improved boundary conditions. Due to the importance of Brownian motion and thermophoresis effects, concentration boundary layer of nanoparticles was considered in their study. Aziz et al. [5] have presented nanofluid natural convection boundary layer flow over a vertical plate subject to the convective boundary conditions. Other studies of the recent evolutions in nanofluid technology have been analyzed and are available in [6–9].

Lately, various investigations have been communicated extending Buongiorno's model for the magnetic nanofluid dynamics, which are essentially helpful in biomedicine, magnetic cell separation, cancer treatment, etc. Bég and Ferdows [10] performed a numerical study to discuss the influence of magnetic field on nanofluid flow from an exponential stretching sheet. Ferdows et al. [11] investigated the unsteady MHD free convective and nanofluid flow from a radiate stretching surface. Sudarsana Reddy et al. [12] reported the influence of magnetic field and chemical reaction on nanofluids over a vertical cone. Ruchika et al. [13] have presented the influence of velocity and thermal slip effects on MHD boundary layer flow of nanofluid over an inclined cylinder. Rashad [14, 15] analyzed the MHD slip flow of a nanofluid past a radiate edge and stretching surface, respectively.

Presently many researchers are concentrating on exploration of non-Newtonian liquids, because non-Newtonian fluids have multidisciplinary applications in modern industrial and technological products. Few examples of non-Newtonian materials include food, ketchup, shampoos, slurries, granular suspension, paper pulp,

***Corresponding Author: G.K. Ramesh,** Department of Mathematics, K.L.E Society's J.T. College, Gadag-582102, Karnataka, India, E-mail: gkrmaths@gmail.com, Ph: +91 9900981204
K. Ganesh Kumar, B.J. Gireesha, Department of Studies and Research in Mathematics, Kuvempu University, Shankaraghatta-577 451, Shimoga, Karnataka, India
A.M. Rashad, Department of Mathematics, Aswan University, Faculty of Science, Aswan, 81528, Egypt

paints, polymer solutions, certain oils, and clay coatings. All the features of non-Newtonian liquids cannot be distinguished by a single mathematical relationship. In view of the above applications Nadeem et al. [16] contemplated the two-dimensional enduring incompressible Oldroyd-B nanofluid stream past an extending sheet. Later they [17, 18] broadened their work on a Jeffrey and Maxwell liquid model. Noor et al. [19] examined the mixed convection boundary layer flow of a micropolar fluid almost a stagnation point along a vertical extending sheet within the sight of nano-particles and slip conditions. Ali and Hayat [20] intoruduced analytical solution for the flow of a Carreau fluid in an asymmetric channel. Olajuwon [21] investigated the convective heat transfer in a MHD Carreau fluid over a vertical radiate plate. Hayat et al. [22, 23] studied the boundary layer flow of Carreau fluid over a stretching surface with convective boundary conditions. As of late numerous analysts [24–34] have studied and discussed about the impacts of slips impacts and nonlinear type of thernmal radiation in the flow of non-Newtonian liquids.

The present problem addresses the impacts of multiple slips, Brownian motion and thermophoresis on MHD flow of Carreau nanofluid over a radiate stretching sheet. The transformed boundary layer equations which represent the flow, temperature and concentration are solved numerically using Runge-Kutta-Fehlberg method of fourth–fifth order using shooting technique. Also comparisons of present result with previously published works was done and are found in excellent agreement.

2 Mathematical formulation

We considered the steady-state incompressible Carreau nanoliquid flow over a stretchable sheet. The x-axis is along the sheet and y-axis normal to it. Here the flow generation is because of linear stretching of surface with distance x, i.e. $U_w = bx$. A constant magnetic field with strength B_0 is implemented in transverse flow direction. $T_w$is the surface temperature at wall and C_w the solutal concentration. At larger distance from surface, temperature and nanoparticle concentration is represented by T_∞ and C_∞ respectively.

The continuity, momentum, energy and concentration expressions are described as

$$\frac{\partial u}{\partial x} + \frac{\partial v}{\partial y} = 0, \tag{1}$$

$$u\frac{\partial u}{\partial x} + v\frac{\partial u}{\partial y} = \nu\frac{\partial^2 u}{\partial y^2} + \frac{3(n-1)}{2}\Gamma^2\frac{\partial^2 u}{\partial y^2}\left(\frac{\partial u}{\partial y}\right)^2 - \frac{\sigma B_0^2}{\rho}u, \tag{2}$$

$$u\frac{\partial T}{\partial x} + v\frac{\partial T}{\partial y} = \alpha\frac{\partial^2 T}{\partial y^2} + \tau\left[D_B\frac{\partial c}{\partial y}\frac{\partial T}{\partial y} + \frac{D_T}{T_\infty}\left(\frac{\partial T}{\partial y}\right)^2\right] - \frac{\partial q_r}{\partial y}, \tag{3}$$

$$u\frac{\partial C}{\partial x} + v\frac{\partial C}{\partial y} = D_B\frac{\partial^2 C}{\partial y^2} + \frac{D_T}{T_\infty}\frac{\partial^2 T}{\partial y^2}, \tag{4}$$

with the relevant boundary conditions (see Ibrahim and Shankar [24])

$$u = u_w, \quad v = 0, \quad T = T_w + K_1\frac{\partial T}{\partial y}, \quad C = C_w + K_2\frac{\partial C}{\partial y} \text{ at } y = 0,$$

$$u \to 0, \quad T \to T_\infty, \quad C \to C_\infty \text{ as } y \to \infty, \tag{5}$$

where the velocity components are presented by u and v, respectively , α for thermal diffusivity, $\nu = \frac{\mu}{\rho}$ for kinematic viscosity, ρ for density of fluid, σ for electrical conductivity, τ for ratio of effective heat capacity of the nanoparticle material to the heat capacity of the fluid, K_1 and K_2 for thermal and concentration slip factor, $D_B$for Brownian diffusion coefficient and D_T for thermophoresis diffusion coefficient, q_r for radiative heat flux. Radiation heat flux q_r via Rosseland approximation can be set in the form:

$$q_r = -\frac{4\sigma^*}{3k^*}\frac{\partial T^4}{\partial y} = -\frac{16\sigma^*}{3k^*}T^3\frac{\partial T}{\partial y} \tag{6}$$

where σ^* for Stefan–Boltzmann constant and k^* for mean absorption coefficient.

The energy equation with radiation heat flux takes the form

$$u\frac{\partial T}{\partial x} + v\frac{\partial T}{\partial y} = \frac{\partial}{\partial y}\left[\left(\alpha + \frac{16\sigma^* {T_\infty}^3}{3k^*}\right)\frac{\partial T}{\partial y}\right] + \tau\left[D_B\frac{\partial c}{\partial y}\frac{\partial T}{\partial y} + \frac{D_T}{T_\infty}\left(\frac{\partial T}{\partial y}\right)^2\right]. \tag{7}$$

For the mathematical analysis of problem, we use the following transformation

$$u = bxf'(\eta), \; v = -\sqrt{b\nu}\,f(\eta), \; \eta = \sqrt{\frac{b}{\nu}}y,$$

$$T = T_\infty\left(1 + (\theta_w - 1)\,\theta(\eta)\right), \quad \phi(\eta) = \frac{C - C_\infty}{C_w - C_\infty}, \tag{8}$$

where $\theta_w = \frac{T_w}{T_\infty}$, $\theta_w > 1$ being the temperature ratio parameter.

After utilizing equation (8), equation (1) is satisfied identically and equations (2), (4) and (7) takes the following form

$$f'''(\eta) - \left(f'(\eta)\right)^2 + f''(\eta) f(\eta) + 3\frac{(n-1)}{2} We f''(\eta)^2 f'''(\eta) - M f'(\eta) = 0, \tag{9}$$

$$\left(1 + R\frac{d}{d\eta}(1 + (1+\theta_w)\theta)^3\right)\theta''(\eta) + Prf\theta' + Nb\theta'\phi' + Nt\,\theta'^2 = 0, \tag{10}$$

$$\phi'' + LePr f \phi' + \frac{Nt}{Nb}\theta'' = 0, \tag{11}$$

with the boundary conditions

$$f = 0, \quad f' = 1, \quad \theta(0) = 1 + B\theta', \quad \phi(0) = 1 + D\phi' \text{ at } \eta = 0$$

$$f' = 0, \quad \theta \to 0, \quad \phi \to 0 \quad \text{as } \eta = \infty, \tag{12}$$

where $M = \frac{\sigma B_0^2}{\rho b}$ for magnetic parameter, $B = K_1\sqrt{\frac{\nu}{b}}$ and $D = K_2\sqrt{\frac{\nu}{b}}$ represents thermal and concentration slip parameters, n for power law index parameter, $We = \frac{\Gamma^2 b U_w}{\nu}$ for Weissenberg number, $Pr = \frac{\nu}{\alpha}$ for Prandtl number, $R = \frac{16\sigma^* T_\infty^3}{3kk^*}$ for radiation parameter, $Le = \frac{\alpha}{D_B}$ for Lewis number, $Nb = \frac{\tau D_B (C_w - C_\infty)}{\nu}$ for Brownian motion parameter, $Nt = \frac{\tau D_T (T_w - T_\infty)}{T_\infty \nu}$ for thermophoresis parameter.

The physical quantities of interest like skin friction coefficient (C_f) local Nusselt number (Nu_x) and local Sherwood number (Sh_x) are

$$c_f = \frac{\tau_w}{\rho U_w^2}, \; Nu_x = \frac{U_w q_w}{kb(T_w - T_\infty)} \text{ and } Sh_x = \frac{U_w q_m}{ab(C_w - C_\infty)},$$

where

$$\tau_w = \mu_0\left(\frac{\partial u}{\partial y} + \frac{n-1\,\Gamma^2}{2}\left(\frac{\partial u}{\partial y}\right)^3\right)_{\eta=0} \quad q_w = -k\frac{\partial T}{\partial y}\,|_{y=0}$$

$$\text{and } q_w = -D\frac{\partial C}{\partial y}\,|_{y=0},$$

Dimensionless form of local skin friction coefficient (C_f), local Nusselt number (Nu_x) and local Sherwood number (Sh_x) are

$$\sqrt{Re_x}C_f = \left[f''(0) + \frac{(n-1)\,We}{2}\left(f''(0)\right)^3\right],$$

$$\frac{Nu_x}{Re^{\frac{1}{2}}} = -\left[1 + R\,\theta_w^3\right]\theta'(0)$$

and

$$\frac{Sh_x}{Re^{\frac{1}{2}}} = -\phi'(0),$$

where the local Reynolds number $Re_x = \frac{u_w^2(x)}{a\nu}$.

3 Numerical Method

Equations (9) to (11) together with the boundary conditions (12) form highly non-linear ordinary differential equations. The reduced set of non-linear ordinary differential equations is solved numerically using Shooting method along with Runge-Kutta-Fehlberg fourth-fifth order scheme. In algebraic package Maple, the Shooting method is implemented as an algorithm called 'shoot'. This Maple software has been well tested for its accuracy and robustness and this has been used to solve a wide range of non-linear problems. It is most important to choose an appropriate finite value of η_∞. In this method, a suitable finite value of η_∞ is considered as η_6 in such way that the boundary conditions defined at infinity satisfy asymptotically. In addition, the relative error tolerance to 10^{-6} is considered for convergence and the step size is chosen as $\Delta\eta = 0.001$. Further it is important to mention that as finding the solutions of velocity, temperature and concentration, the CPU time to estimate the values of velocity (1.32 sec) is much less than the CPU time to evaluate the values of temperature (1.74 sec) and the CPU time for concentration is 1.96 sec.

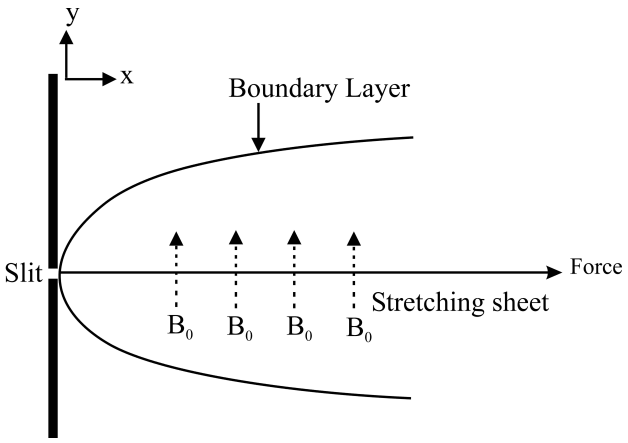

Fig. 1: Schematic representation of the flow diagram.

4 Results and discussion

In this section, the influences several physical parameters on the velocity, temperature and nanoparticle concentration profiles are analyzed graphically with tabulated results and relevant discussions. Eqs. (7)- (9) with the boundary conditions (10) are solved numerically with fifth-order Runge-Kutta Scheme using shooting scheme for the values of physical parameters like

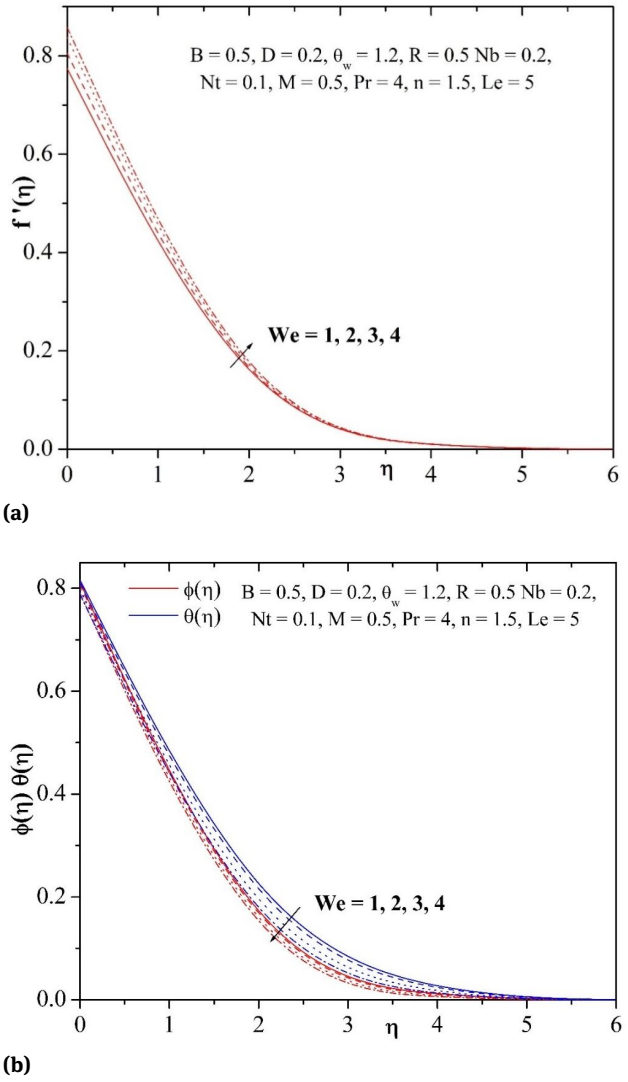

Fig. 2: (a) Influence of *We* on velocity profile. (b) Influence of *We* on temperature and concentration profiles.

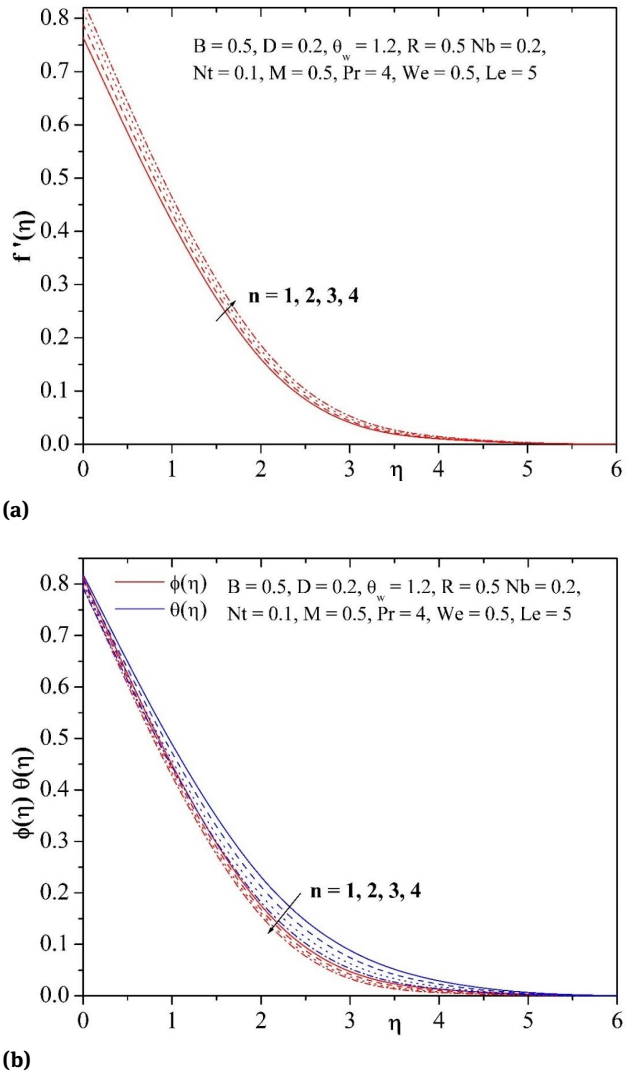

Fig. 3: (a) Influence of n on velocity profile. (b)Influence of n on temperature and concentration profiles.

We, n, M, B, D, Nb, Nt, R, θ_w, Pr, Le. The results are reported graphically in Figures 2-5 and conclusions are drawn to analyze the effects of various physical quantities of interest on velocity, temperature and concentration profiles as well as the local skin friction, heat transfer rate and mass transfer rates that have significant effects. Comparisons, displayed in Tables 1 and 2, the present results with previously published works are performed and excellent agreements have been obtained.

Fig. 2(a)-3(c) show the profiles for velocity $f'(\eta)$, temperature $\theta(\eta)$ and concentration $\varphi(\eta)$ for different values of Weissenberg number We and power law index n. It is observed that an increase in the Weissenberg number We and power law index n leads to increase the fluid velocity and to decrease both the temperature and concentration profiles. The influence of magnetic field parameter M on velocity, temperature and concentration profiles in the boundary layer is displayed in Figs. 4(a)-4(c). It is noticed from these figures that the hydrodynamic boundary layer thickness decelerates whilst thermal boundary layer thickness and solutal boundary layer thickness elevates with enhance in the values of M. This is because of the fact that, the presence of magnetic field in an electrically conducting fluid produces a force called Lorentz force, this force acts versus the flow trend causes the depreciation in velocity profiles Fig. 4(a), and at the same time, to overcome the drag force imposed by the Lorentzian retardation the fluid has to result in extra work; this additional work can be converted into thermal energy which enhances the temperature of the fluid Fig. 4(b) and also enhances the concentration profiles Fig. 4(c).

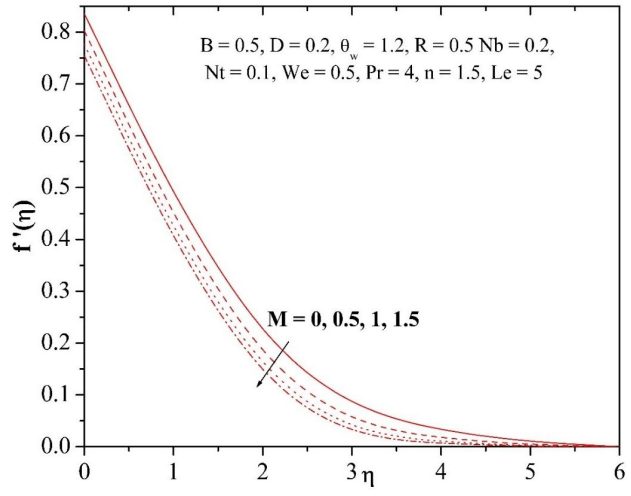

(a)

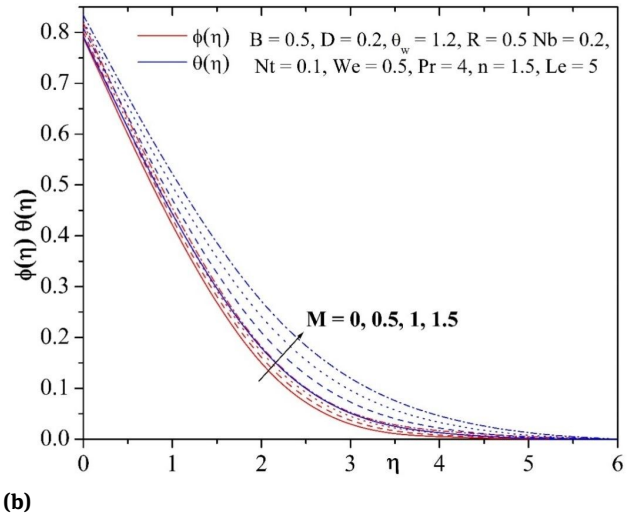

(b)

Fig. 4: (a) Influence of M on velocity profile. (b) Influence of M on temperature and concentration profiles.

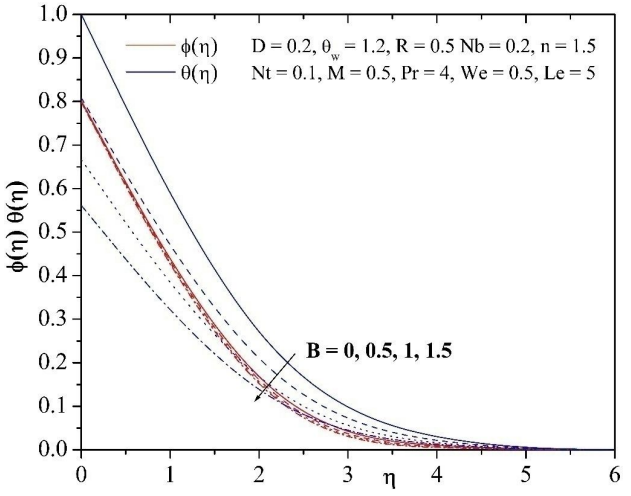

(a)

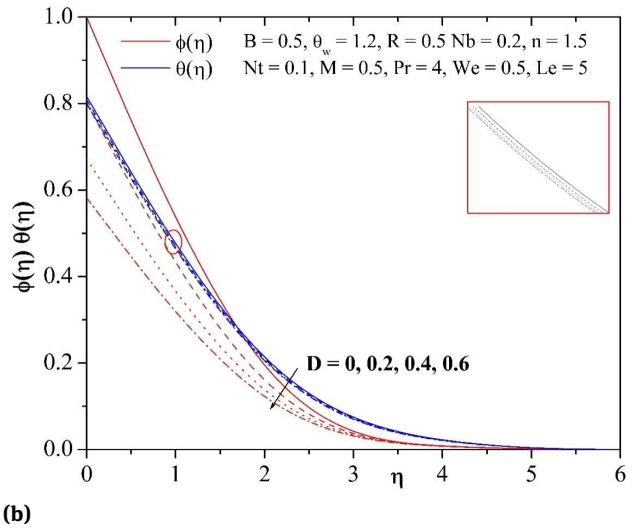

(b)

Fig. 5: (a) Influence of B on temperature and concentration profiles. (b) Influence of D on temperature and concentration profiles.

Effects of thermal slip parameter B and solutal slip parameter D on the dimensionless temperature, nanoparticle volume fraction profiles are displayed in Figs. 5(a)-5(b). As the thermal slip parameter B and solutal slip parameter D enhances, both the temperature and nanoparticle volume fraction reduces near the plate surface. This elucidates that temperature and nanoparticle volume fraction near the surface reduces to a minimum with strong thermal and solutal slips and achieves a maximum with no thermal and solutal slip effects. This behavior happens due to fluid in the boundary layer being insensitive toward the heating effects of the plate surface and hence diminished heat and mass will be transferred from the surface to the nanofluid body.

Fig. 6(a) demonstrates that due to increasing the value of the Brownian parameter Nb, the temperature profile boosts, whereas the opposite trend is noted for the concentration profile. Therfore, the thermal boundary layer thickness increases, whereas the concentration boundary layer thickness decreases. This is due to the fact that the kinetic energy of the nanoparticles promotes due to the strength of this chaotic motion and as a result, the fluids temperature raises. This is because the Brownian motion at the nanoscale and the molecular levels is an important mechanism of the nanoscale level that dominates the thermal behaviors. In systems using nanofluids, the Brownian motion takes place because of the size of nanoparticles which can change the properties of heat transfer. As the scale size of particles approaches the scale of nanometer, the particles Brownian motion and its result on the surrounding liquids play a pivotal role in heat transfer characteristics.

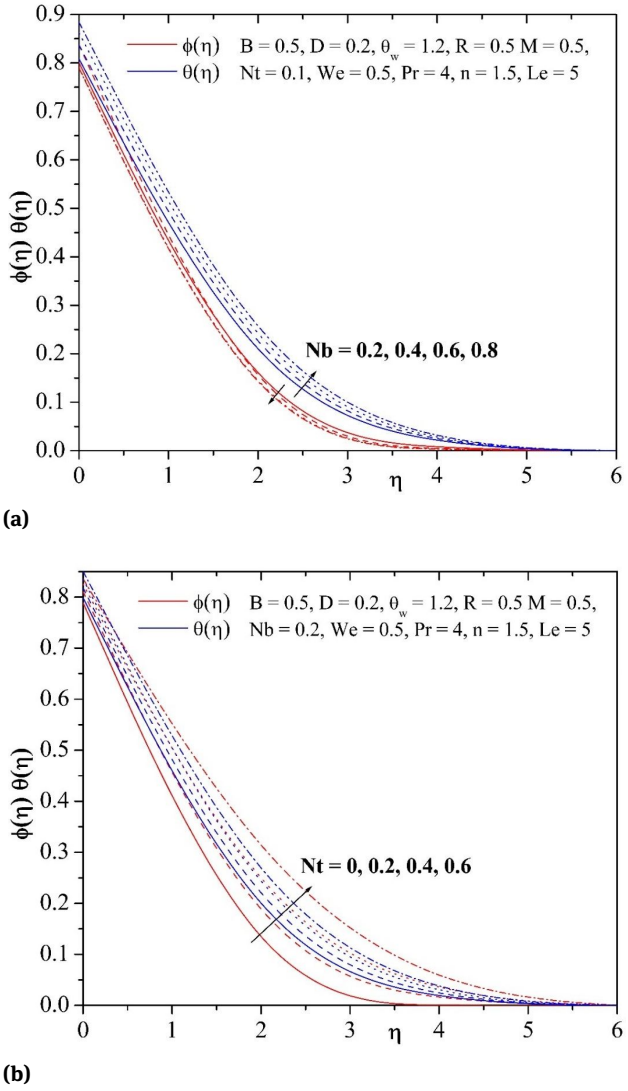

Fig. 6: (a) Influence of *Nb* on temperature and concentration profiles. (b) Influence of *Nt* on temperature and concentration profiles.

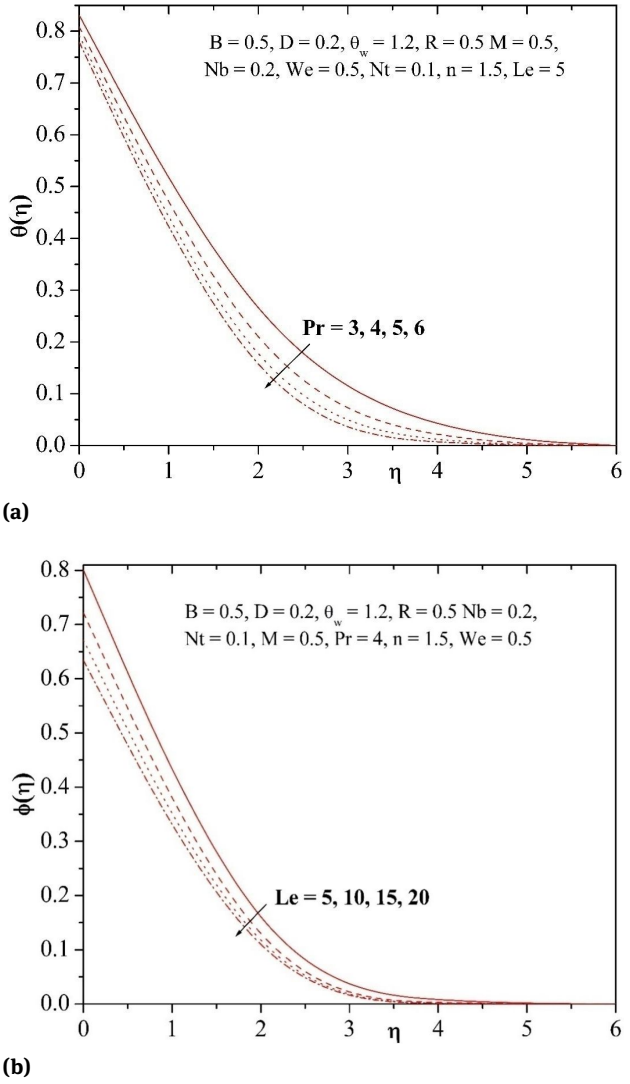

Fig. 7: (a) Influence of *Pr* on temperature profile. (b) Influence of *Le* on concentration profile.

Fig. 6(b) reveals the impact of the thermophoresis parameter *Nt* on the temperature and the concentration of nanoparticle profiles. It is noticed that the temperature profile and the concentration of nanoparticle increase with increasing *Nt* . This is because diffusion penetrates profounder into the fluid due to boosting values of *Nt* which produces the thickening of the thermal boundary layer as well as the concentration boundary layer.

The significance of Prandtl number *Pr* on the temperature profiles is depicted in Fig. 7(a). It is noted that the temperature distributions diminish when *Pr* values increases. By definition, Prandtl number is defined as the ratio of momentum diffusivity to the thermal diffusivity, raising the values of *Pr* means higher momentum diffusivity or lesser thermal diffusivity which results in the reduction in the thermal boundary layer thickness. Fig. 7(b) presents the concentration profiles for different values of and Lewis number *Le*. It is observed that concentration distributions decelerate with elevating values of *Le* in the entire boundary layer region. The Lewis number defines the ratio of thermal diffusivity to mass diffusivity. Elevating the Lewis number means a higher thermal diffusivity or lower mass diffusivity and this provides thinner concentration boundary layer.

Figs. 8(a)-8(b) illustrate the influences of temperature ratio parameter θ_w and radiation parameter R on the temperature profiles, respectively. It is seen that as the values of θ_w rises the fluid temperarure diminishes significantly and this depreciation is more near the surface than in the far-field regime (free stream of the boundary layer). Fur-

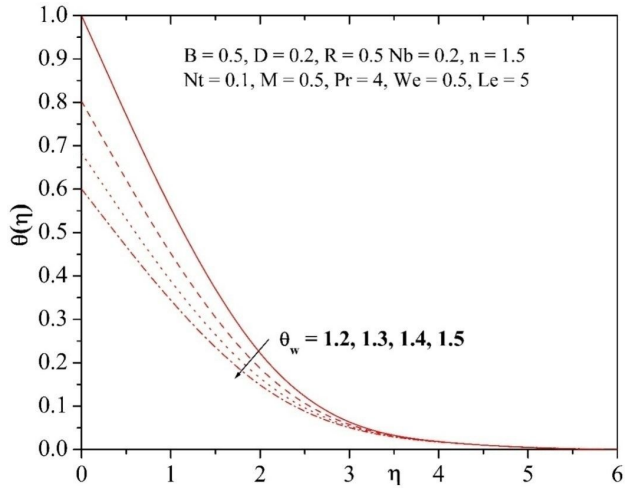

(a)

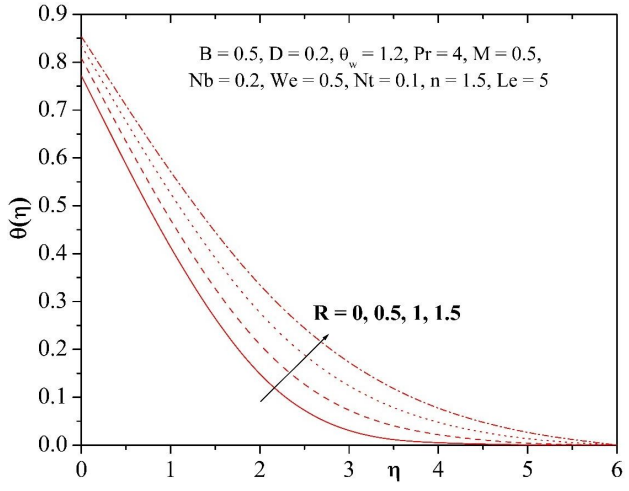

(b)

Fig. 8: (a) Influence of θ_w on temperature profile. (b) Influence of R on temperature profile.

thermore, it is perceived from Fig. 8(b) that as the values of radiation parameter R increases the temperature profiles are also enhanced. This is because of the fact that the mean absorption coefficient reduces with increasing values of radiation parameter; as a result the thermal boundary layer thickness of the nanofluid is promotes.

The variations of skin-friction coefficient $-f''(0)$, Nusselt number $-\theta'(0)$ and Sherwood number $-\phi'(0)$ for diverse values of governing parameters are calculated and summarized in Tables 3-4. It is clear from these tables that the heat and mass transfer rates are both decelerates, whereas the skin-friction coefficient enhances with the increasing values of magnetic parameter M. It is also evident that the increasing of power law index n leads to escalate all the skin-friction coefficient, Nusselt and Sherwood numbers in the entire nanofluid regime, but reverse trend

Table 1: Comparison results for the function $-f''(0)$ for several values of M in the case, $We = 0$, $and\ n = 0$, (absence of temperature and concentration).

	Cortell [32]	Ramesh et al. [33]	Present result
M	$-f''(0)$	$-f''(0)$	$-f''(0)$
0	1.000	1.000	1.00006
0.2	1.095	1.095	1.09546
0.5	1.224	1.224	1.22475
1	1.414	1.414	1.41421
1.2	1.483	1.483	1.48324
1.5	1.581	1.581	1.58114
2	1.732	1.732	1.73205

Table 2: Comparison of the result for Nusselt number $-\theta'(0)$ in the absence of We, θ_w, R, B, D.

Pr	Khan and Pop [34]	Present result (RKF-45 method)
0.7	0.4539	0.45357
2	0.9113	0.91135
7	1.8954	1.89539
20	3.3539	3.35387
70	6.4621	6.46209

is noted with rising values of Weissenberg number We. Moreover, increasing the thermal slip parameter B generates a growth in values of Sherwood number and deceleration in the Nusselt number, while the opposite behaviors occurs with the increment in the solutal slip parameter D. Physically, as the thermal slip increases, this decelerates the capability of the nanofluid in the boundary layer to feel the heating impact of the plate surface, and hence, heat transfer rate reduces. Furthermore, the heat and mass transfer are enhanced when Brownian parameter Nb increased, whereas, they are depreciated with higher values of the thermophoresis parameter Nt. It is observed that both Nusselt number enhances and Sherwood numbers diminishes as Prandtl number Pr increases while the reverse trend happens with improving values of Lewis number Le.

Table 3: Variation of skin friction coefficient, Nusselt number and Sherwood number for different physical parameters.

M	We	n	$-\sqrt{Re_x}C_f$	$-\frac{Nu}{\sqrt{Re_x}}$	$-\frac{Sh}{\sqrt{Re_x}}$
0			0.2708	0.7742	1.0521
0.5			0.4255	0.7134	0.9961
1			0.5475	0.6629	0.9493
	0		0.4324	0.7284	1.0112
	1		0.3234	0.7147	0.9880
	2		0.1217	0.7045	0.9801
		0	-0.9778	0.6983	0.9707
		1	0.1258	0.7284	1.0112
		2	1.2211	0.7573	1.0398

Table 4: Variation of Nusselt number and Sherwood number for different physical parameter.

B	D	θ_w	Le	Nb	Nt	Pr	R	$-\frac{Nu}{\sqrt{Re_x}}$	$-\frac{Sh}{\sqrt{Re_x}}$
0								0.8222	0.9894
0.5								0.7134	0.9961
1								0.6210	1.0024
	0							0.6847	1.2686
	0.2							0.7134	0.9961
	0.4							0.7324	0.8199
		1.2						0.7144	0.9961
		1.3						0.7221	1.0050
		1.4						0.7325	1.0125
			5					0.7097	0.9961
			10					0.7107	1.3919
			15					0.7134	1.6437
				0.2				0.6824	0.8760
				0.4				0.6123	0.9526
				0.6				0.5436	1.2344
					0			0.7500	1.0548
					0.2			0.6786	0.9468
					0.4			0.6144	0.8714
						3		0.6298	1.0037
						4		0.7134	0.9961
						5		0.7760	0.9907
							0	0.4561	0.9845
							0.5	0.7134	0.9961
							1	0.9011	1.0051

Finally, It is seen that with the higher values of radiation parameter R and temperature ratio parameter θ_w, both the Nusselt and Sherwood numbers elevate in the boundary layer regime.

5 Conclusion

The impacts of multiple slips and thermal radiation on MHD flow of Carreau nanofluid over a stretching sheet with thermal radiation are numerically analyzed in this article. The slip of the heat and mass transfer in this problem is because of Brownian motion and thermophoresis. In the mathematical modeling of the problem effect of Carreau nanofluid, the dynamic effects of nanoparticles, thermophoresis and Brownian motion are taken into the account. The effects of different parameters on velocity, temperature and concentration profiles, as well as skin-friction coefficient, Nusselt number and Sherwood number were analyzed. The results of present study can be summarized as follows:

- The Nusselt and Sherwood numbers deteriorate, whereas the skin-friction coefficient is elevates with the higher values of magnetic parameter M.
- With the higher values of values of thermophoretic parameter Nt, the heat and mass transfer are reduced.
- A rise in Brownian motion parameter Nb improves the heat and mass transfer rates.
- All the skin-friction coefficient, Nusselt and Sherwood numbers depreciate when Weissenberg number We is upgrades, whereas, they elevates as the power law index $n$increases.
- Increasing both the radiation parameter R and temperature ratio parameter θ_w, both the Nusselt and Sherwood numbers elevate in the boundary layer regime.

Acknowledgement: The authors are very much thankful to the editor and referee for their encouraging comments and constructive suggestions to improve the presentation of this manuscript.

Nomenclature

b Constants
B_0 magnetic field
B and D thermal and solutal slip parameter

C nanoparticle volume fraction
C_w concentration at the wall
C_∞ ambient nanofluid volume fraction
C_f skin friction coefficient
c_p specific heat coefficient
K_1 and K_2 slip factor
T fluid temperature
T_w surface temperature
T_∞ ambient surface temperature
D_B Brownian diffusion coefficient
D_T thermophoretic diffusion coefficient
k thermal conductivity
k^* mean absorption coefficient
Le Lewis number
Nb Brownian motion parameter
Nt thermophoresis parameter
Nu_x local Nusselt number
n Power law index
Pr Prandtl number
q_r radiative heat flux
q_w heat flux
q_m mass flux
R radiation parameter
Re_x local Reynolds number
Sh_x local Sherwood number
u, v velocity components
U_w stretching sheet
We Weissenberg number
x, y Coordinates

Greek symbols

θ dimensionless temperature
θ_w temperature ratio parameter
ϕ dimensionless nanoparticle volume fraction
ν Kinematic viscosity of the fluid
μ coefficient of fluid viscosity
σ^* Stefan–Boltzmann constant
τ ratio of the effective heat capacity of the nanoparticle to that of an ordinary fluid
τ_w shear stress along the wall
α Prandtl parameter
β elastic parameter
α_1 thermal diffusivity of the fluid
ρ fluid density

References

[1] S. K. Das, S. U. S. Choi, W. Yu and T. Pradeep, Nanofluids-science and technology, John Wiley & Sons Publishers, Hoboken, (2007).
[2] S. U. S. Choi, Enhancing thermal conductivity of fluids with nanoparticle. in: D.A. Siginer, H.P. Wang (Eds.), Developments and Applications of Non-Newtonian Flows, ASME FED, vol. 231/MD 66 (1995) 99-105.
[3] A.V. Kuznetstov and D.A. Neild, Natural convective boundary-layer flow of a nanofluid past a vertical plate: A revised model, International journal of thermal sciences, 77(2014) 126-129.
[4] J. Buongiorno, Convective transport in nanofluids, ASME Journal of Heat Transfer, 128 (2006) 240-250.
[5] A. Aziz and W.A. Khan, Natural convective boundary layer flow of a nanofluid past a convectively heated vertical plate, Int. J. Therm. Sci., 52(2012) 83-90.
[6] A. J. Chamkha, M. Modather, S. M. M. EL-Kabeir and A. M. Rashad, Radiative effects on boundary-layer flow of a nanofluid on a continuously moving or fixed permeable surface, Recent Patents on Mechanical Engineering, 5 (3) (2012) 176-183.
[7] G. K. Ramesh, B. J. Gireesha T. Hayat and A. Alsdedi, Stagnation point flow of Maxwell fluid towards a permeable surface in the presence of nanoparticles, Alexandria Engineering Journal, 53(2016) 857-865.
[8] A. J. Chamkha and A. M. Rashad, Natural convection from a vertical permeable cone in nanofluid saturated porous media for uniform heat and nanoparticles volume fraction fluxes, International Journal of Numerical Methods for Heat and Fluid Flow, 22(8) (2012) 1073-1085.
[9] A. J. Chamkha, S. Abbasbandy, A. M. Rashad and K. Vajravelu, Radiation effects on mixed convection about a cone embedded in a porous medium filled with a nanofluid, Meccanica, 48 (2013) 275-285.
[10] O. A. Bég and M. Ferdows, Explicit numerical simulation of magnetohydrodynamic nanofluid flow from an exponential stretching sheet in porous media. Appl Nanosci 2013; 1-15. DOI: 10.1007/s13204-013-0275-0.
[11] M. Ferdows, M. S. Khan, O. A. Bég, M. A. K. Azad and M. M. Alam, Numerical study of transient magnetohydrodynamic radiative free convection nanofluid flow from a stretching permeable surface. Proc IMechE, Part E: J Process Mechanical Engineering. Epub ahead of print 25 September 2013. DOI: 10.1177/0954408913493406.
[12] P. Sudarsana Reddy and K. V. Suryanarayana Rao, MHD natural convection heat and mass transfer of Al2O3 - water and Ag - water nanofluids over a vertical cone with chemical reaction, Procedia Engineering, 127(2015)476-484.
[13] D. Ruchika, Puneet Rana and Lokendra Kumar, MHD mixed convection nanofluid flow and heat transfer over an inclined cylinder due to velocity and thermal slip effects: Buongiorno's model, Powder Technology, 288(2016)140-150.
[14] A. M. Rashad, Impact of thermal radiation on MHD slip flow of a ferrofluid over a nonisothermal wedge, Journal of Magnetism and Magnetic Materials, 422 (2017) 25-31.
[15] A. M. Rashad, Impact of anisotropic slip on transient three dimensional MHD flow of ferrofluid over an inclined radiate stretching surface, Journal of the Egyptian Mathematical Soci-

ety, (In Press).
[16] S. Nadeem, Rizwan Ul Haq , N. S. Akbar, C. Lee and Z. H. Khan, Numerical study of boundary layer flow and heat transfer of Oldroyd-B nanofluid towards a stretching sheet, PLoS ONE 8(8)(2013) e69811. https://doi.org/10.1371/journal.pone.0069811.
[17] S. Nadeem, Rizwan Ul Haq and Z. H. Khan, Numerical solution of non-Newtonian nanofluid flow over a stretching sheet, Applied Nanoscience, 4(5) (2014) 625–631.
[18] S. Nadeem, Rizwan Ul Haq and Z. H. Khan, Numerical study of MHD boundary layer flow of a Maxwell fluid past a stretching sheet in the presence of nanoparticles, Journal of the Taiwan Institute of Chemical Engineers, 45(1)(2014) 121-126.
[19] N.F.M. Noor, Rizwan Ul Haq, S. Nadeem and I. Hashim, Mixed convection stagnation flow of a micropolar nanofluid along a vertically stretching surface with slip effects, Meccanica, 50 (2015) 2007–2022.
[20] N. Ali and T. Hayat, Peristaltic motion of a Carreau fluid in an asymmetric channel Appl. Math. Comput. 193(2007) 535-552.
[21] B. I. Olajuwon, Convection heat and mass transfer in a hydromagnetic Carreau fluid past a vertical porous plate in presence of thermal radiation and thermal diffusion Thermal. Sci. 15(2011) 241-252.
[22] T. Hayat, S. Asad, M. Mustafa and A. Alsaedi, Boundary layer flow of Carreau fluid over a convectively heated stretching sheet, Appl. Math. Comput. 246(2014)12-22.
[23] T. Hayat, M Waqas, S. A. Shehzad, A. AL-Saedi, Stretched flow of Carreau nanofluid with convective boundary condition, PRAMANA-Journal of Physics, 86 (1) (2016)3-17.
[24] W. Ibrahim and B. Shankar, MHD boundary layer flow and heat transfer of a nanofluid past a permeable stretching sheet with velocity, thermal and solutal slip boundary conditions Computers and fluids, 75(2013) 1-10.
[25] S.K.Parida, S.Panda, and B.R.Rout, MHD boundary layer slip flow and radiative nonlinear heat transfer over a flat plate with variable fluid properties and thermophoresis, Alexandria Engineering Journal, 54(4)(2015)941-953.
[26] G.K. Ramesh, Numerical study of the influence of heat source on stagnation point flow towards a stretching surface of a Jeffrey nanoliquid, Journal of Engineering, 2015 (2015), Article ID 382061, 10 pages http://dx.doi.org/10.1155/2015/382061
[27] Muhammad A Imran, S. Sarwar and Muhammad Imran, Effects of slip on free convection flow of Casson fluid over an oscillating vertical plate, Boundary Value Problems, 2016 (30)(2016). https://doi.org/10.1186/s13661-016-0538-2
[28] Y. S. Daniel, Z.A.Aziz, Z.Ismail and F. Salah, Effects of slip and convective conditions on MHD flow of nanofluid over a porous nonlinear stretching/shrinking sheet, Australian Journal of Mechanical Engineering (2017)1-17. http://dx.doi.org/10.1080/14484846.2017.1358844
[29] R. A. Shah, T. Abbas, M. Idrees and M. Ullah, MHD Carreau fluid slip flow over a porous stretching sheet with viscous dissipation and variable thermal conductivity, Boundary Value Problems, 2017(94)(2017)
[30] K.Ganesh Kumar, N. Rudraswamy, B.J. Gireesha and M.R. Krishnamurthy, Influence of nonlinear thermal radiation and viscous dissipation on three-dimensional flow of Jeffrey nano fluid over a stretching sheet in the presence of Joule heating. Nonlinear Engineering, 6(3) (2017) 207-219.
[31] K.Ganesh Kumar, G.K.Ramesh, B.J.Gireesha and R.S.R.Gorla, Characteristics of Joule heating and viscous dissipation on three-dimensional flow of Oldroyd B nanofluid with thermal radiation, Alexandria Engineering Journal, (2017). https://doi.org/10.1016/j.aej.2017.06.006
[32] R. Cortell, A note on magnetohydrodynamic flow of a power-law fluid over a stretching sheet. Appl. Math. Comput. 168 (2005)557–566
[33] G. K. Ramesh, B. J. Gireesha and C. S. Bagewadi, Stagnation point flow of a MHD dusty fluid towards a stretching sheet with radiation, Afrika Matematika, 25(1) (2014) 237-249.
[34] W. A. Khan and I, Pop, Boundary-layer flow of a nanofluid past a stretching sheet. Int. J Heat Mass Transfer, 53(2010)2477–2483.